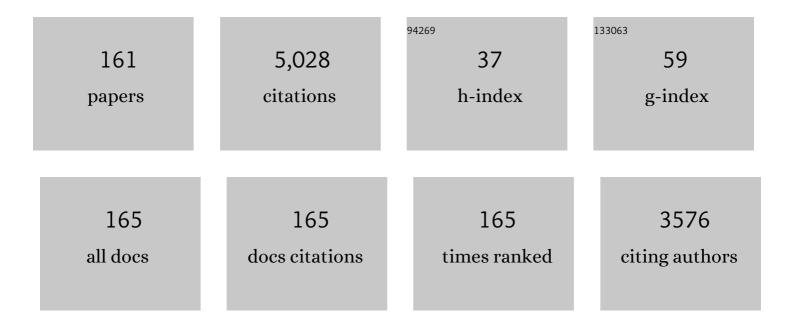
## Xue-Zhang Xiao

List of Publications by Year in descending order

Source: https://exaly.com/author-pdf/9113303/publications.pdf Version: 2024-02-01



#	Article	IF	CITATIONS
1	All-temperature batteries enabled by fluorinated electrolytes with non-polar solvents. Nature Energy, 2019, 4, 882-890.	19.8	557
2	Novel 1D carbon nanotubes uniformly wrapped nanoscale MgH2 for efficient hydrogen storage cycling performances with extreme high gravimetric and volumetric capacities. Nano Energy, 2019, 61, 540-549.	8.2	124
3	ZIF-67 derived Co@CNTs nanoparticles: Remarkably improved hydrogen storage properties of MgH2 and synergetic catalysis mechanism. International Journal of Hydrogen Energy, 2019, 44, 1059-1069.	3.8	111
4	Lowâ€Temperature Combustion‣ynthesized Nickel Oxide Thin Films as Holeâ€Transport Interlayers for Solutionâ€Processed Optoelectronic Devices. Advanced Energy Materials, 2014, 4, 1301460.	10.2	110
5	Enhanced hydrogen storage properties of MgH <sub>2</sub> with numerous hydrogen diffusion channels provided by Na <sub>2</sub> Ti <sub>3</sub> O <sub>7</sub> nanotubes. Journal of Materials Chemistry A, 2017, 5, 6178-6185.	5.2	89
6	Excellent catalysis of TiO <sub>2</sub> nanosheets with high-surface-energy {001} facets on the hydrogen storage properties of MgH <sub>2</sub> . Nanoscale, 2019, 11, 7465-7473.	2.8	89
7	Facile synthesis of Co/Pd supported by few-walled carbon nanotubes as an efficient bidirectional catalyst for improving the low temperature hydrogen storage properties of magnesium hydride. Journal of Materials Chemistry A, 2019, 7, 5277-5287.	5.2	88
8	Superior de/hydrogenation performances of MgH2 catalyzed by 3D flower-like TiO2@C nanostructures. Journal of Energy Chemistry, 2020, 46, 191-198.	7.1	88
9	Transition metal (Co, Ni) nanoparticles wrapped with carbon and their superior catalytic activities for the reversible hydrogen storage of magnesium hydride. Physical Chemistry Chemical Physics, 2017, 19, 4019-4029.	1.3	86
10	Novel AgPd hollow spheres anchored on graphene as an efficient catalyst for dehydrogenation of formic acid at room temperature. Journal of Materials Chemistry A, 2016, 4, 657-666.	5.2	75
11	Remarkably Improved Hydrogen Storage Performance of MgH <sub>2</sub> Catalyzed by Multivalence NbH <sub><i>x</i></sub> Nanoparticles. Journal of Physical Chemistry C, 2015, 119, 8554-8562.	1.5	73
12	In situ synthesis of SnO <sub>2</sub> nanoparticles encapsulated in micro/mesoporous carbon foam as a high-performance anode material for lithium ion batteries. Journal of Materials Chemistry A, 2014, 2, 18367-18374.	5.2	64
13	Carbon encapsulated 3D hierarchical Fe3O4 spheres as advanced anode materials with long cycle lifetimes for lithium-ion batteries. Journal of Materials Chemistry A, 2014, 2, 14641-14648.	5.2	62
14	Development of Ti–Cr–Mn–Fe based alloys with high hydrogenÂdesorption pressures for hybrid hydrogen storage vessel application. International Journal of Hydrogen Energy, 2013, 38, 12803-12810.	3.8	61
15	Synergistic Catalytic Activity of Porous Rod-like TMTiO <sub>3</sub> (TM = Ni and Co) for Reversible Hydrogen Storage of Magnesium Hydride. Journal of Physical Chemistry C, 2018, 122, 27973-27982.	1.5	61
16	Excellent synergistic catalytic mechanism of in-situ formed nanosized Mg2Ni and multiple valence titanium for improved hydrogen desorption properties of magnesium hydride. International Journal of Hydrogen Energy, 2019, 44, 1750-1759.	3.8	61
17	Enhanced hydrogen storage capacity and reversibility of LiBH4 nanoconfined in the densified zeolite-templated carbon with high mechanical stability. Nano Energy, 2015, 15, 244-255.	8.2	58
18	Highly synergetic catalytic mechanism of Ni@g-C3N4 on the superior hydrogen storage performance of Li-Mg-B-H system. Energy Storage Materials, 2018, 13, 199-206.	9.5	58

#	Article	IF	CITATIONS
19	Synergistic catalysis in monodispersed transition metal oxide nanoparticles anchored on amorphous carbon for excellent low-temperature dehydrogenation of magnesium hydride. Materials Today Energy, 2019, 12, 146-154.	2.5	57
20	Non-noble trimetallic Cu-Ni-Co nanoparticles supported on metal-organic frameworks as highly efficient catalysts for hydrolysis of ammonia borane. Journal of Alloys and Compounds, 2018, 741, 501-508.	2.8	55
21	Effect of rare earth doping on the hydrogen storage performance of Ti1.02Cr1.1Mn0.3Fe0.6 alloy for hybrid hydrogen storage application. Journal of Alloys and Compounds, 2018, 731, 524-530.	2.8	55
22	Active species of CeAl4 in the CeCl3-doped sodium aluminium hydride and its enhancement on reversible hydrogen storage performance. Chemical Communications, 2009, , 6857.	2.2	54
23	Remarkable hydrogen desorption properties and mechanisms of the Mg <sub>2</sub> FeH <sub>6</sub> @MgH <sub>2</sub> core–shell nanostructure. Journal of Materials Chemistry A, 2015, 3, 5517-5524.	5.2	54
24	Enhanced hydriding–dehydriding performance of 2LiBH4–MgH2 composite by the catalytic effects of transition metal chlorides. Journal of Materials Chemistry, 2012, 22, 20764.	6.7	53
25	Low-Temperature Reversible Hydrogen Storage Properties of LiBH <sub>4</sub> : A Synergetic Effect of Nanoconfinement and Nanocatalysis. Journal of Physical Chemistry C, 2014, 118, 11252-11260.	1.5	51
26	High catalytic efficiency of amorphous TiB2 and NbB2 nanoparticles for hydrogen storage using the 2LiBH4–MgH2 system. Journal of Materials Chemistry A, 2013, 1, 11368.	5.2	47
27	Influence of Ti super-stoichiometry on the hydrogen storage properties of Ti1+xCr1.2Mn0.2Fe0.6 (x=0–0.1) alloys for hybrid hydrogen storage application. Journal of Alloys and Compounds, 2014, 585, 307-311.	2.8	47
28	Catalytic Mechanism of New TiC-Doped Sodium Alanate for Hydrogen Storage. Journal of Physical Chemistry C, 2009, 113, 20745-20751.	1.5	46
29	Improvement on the kinetic and thermodynamic characteristics of Zr1-xNbxCo (xÂ= 0–0.2) alloys for hydrogen isotope storage and delivery. Journal of Alloys and Compounds, 2019, 784, 1062-1070.	2.8	46
30	Effects of NbF5 addition on the de/rehydrogenation properties of 2LiBH4/MgH2 hydrogen storage system. International Journal of Hydrogen Energy, 2012, 37, 13147-13154.	3.8	45
31	Self-templated carbon enhancing catalytic effect of ZrO2 nanoparticles on the excellent dehydrogenation kinetics of MgH2. Carbon, 2020, 166, 46-55.	5.4	45
32	Enhanced Hydridingâ^'Dehydriding Performance of CeAl <sub>2</sub> -Doped NaAlH <sub>4</sub> and the Evolvement of Ce-Containing Species in the Cycling. Journal of Physical Chemistry C, 2011, 115, 2537-2543.	1.5	41
33	Effects of fluoride additives on dehydrogenation behaviors of 2LiBH4Â+ÂMgH2 system. International Journal of Hydrogen Energy, 2012, 37, 1021-1026.	3.8	41
34	Facile preparation of β-/γ-MgH <sub>2</sub> nanocomposites under mild conditions and pathways to rapid dehydrogenation. Physical Chemistry Chemical Physics, 2016, 18, 10492-10498.	1.3	41
35	Significantly improved hydrogen storage properties of NaAlH4 catalyzed by Ce-based nanoparticles. Journal of Materials Chemistry A, 2013, 1, 9752.	5.2	40
36	Microstructure and hydrogen storage properties of Ti10V84â^'xFe6Zrx (x=1–8) alloys. International Journal of Hydrogen Energy, 2010, 35, 3080-3086.	3.8	39

#	Article	IF	CITATIONS
37	Carbon coated sodium-titanate nanotube as an advanced intercalation anode material for sodium-ion batteries. Journal of Alloys and Compounds, 2017, 712, 365-372.	2.8	39
38	Size effect on hydrogen storage properties of NaAlH4 confined in uniform porous carbons. Nano Energy, 2013, 2, 995-1003.	8.2	38
39	Reversible hydrogen storage properties and favorable co-doping mechanism of the metallic Ti and Zr co-doped sodium aluminum hydride. International Journal of Hydrogen Energy, 2008, 33, 64-73.	3.8	36
40	A new strategy for remarkably improving anti-disproportionation performance and cycling stabilities of ZrCo-based hydrogen isotope storage alloys by Cu substitution and controlling cutoff desorption pressure. International Journal of Hydrogen Energy, 2019, 44, 28242-28251.	3.8	36
41	Effect of Mn substitution for Co on the structural, kinetic, and thermodynamic characteristics of ZrCo1â^'Mn (x=0–0.1) alloys for tritium storage. International Journal of Hydrogen Energy, 2017, 42, 28498-28506.	3.8	35
42	Synergistic Effect of LiBH <sub>4</sub> and LiAlH <sub>4</sub> Additives on Improved Hydrogen Storage Properties of Unexpected High Capacity Magnesium Hydride. Journal of Physical Chemistry C, 2018, 122, 2528-2538.	1.5	35
43	Remarkable hydrogen absorption/desorption behaviors and mechanism of sodium alanates in-situ doped with Ti-based 2D MXene. Materials Chemistry and Physics, 2020, 242, 122529.	2.0	35
44	Direct synthesis of nanocrystalline NaAlH4 complex hydride for hydrogen storage. Applied Physics Letters, 2009, 94, 041907.	1.5	34
45	Enhanced low temperature hydrogen desorption properties and mechanism of Mg(BH4)2 composited with 2D MXene. International Journal of Hydrogen Energy, 2019, 44, 24292-24300.	3.8	34
46	An in-depth study on the thermodynamics and kinetics of disproportionation behavior in ZrCo–H systems. Journal of Materials Chemistry A, 2020, 8, 9322-9330.	5.2	34
47	Investigation on Ti–Zr–Cr–Fe–V based alloys for metal hydride hydrogen compressor at moderate working temperatures. International Journal of Hydrogen Energy, 2021, 46, 21580-21589.	3.8	34
48	AuPd Nanoparticles Anchored on Nitrogen-Decorated Carbon Nanosheets with Highly Efficient and Selective Catalysis for the Dehydrogenation of Formic Acid. Journal of Physical Chemistry C, 2018, 122, 4792-4801.	1.5	33
49	Hydriding-dehydriding kinetics and the microstructure of La- and Sm-doped NaAlH4 prepared via direct synthesis method. International Journal of Hydrogen Energy, 2011, 36, 10861-10869.	3.8	32
50	Influence of heat treatment on the microstructure and hydrogen storage properties of Ti10V77Cr6Fe6Zr alloy. Journal of Alloys and Compounds, 2012, 529, 128-133.	2.8	32
51	Development of Ti-Zr-Mn-Cr-V based alloys for high-density hydrogen storage. Journal of Alloys and Compounds, 2021, 875, 160035.	2.8	32
52	SnLi4.4 nanoparticles encapsulated in carbon matrix as high performance anode material for lithium-ion batteries. Nano Energy, 2014, 9, 196-203.	8.2	30
53	Microstructure and hydrogen storage characteristics of nanocrystalline Mg+xwt% LaMg2Ni (x=0–30) composites. International Journal of Hydrogen Energy, 2010, 35, 2786-2790.	3.8	29
54	Highly dispersed metal nanoparticles on TiO2 acted as nano redox reactor and its synergistic catalysis on the hydrogen storage properties of magnesium hydride. International Journal of Hydrogen Energy, 2019, 44, 15100-15109.	3.8	29

#	Article	IF	CITATIONS
55	The hydrogen storage properties and microstructure of Ti-doped sodium aluminum hydride prepared by ball-milling. International Journal of Hydrogen Energy, 2007, 32, 2475-2479.	3.8	28
56	Enhanced hydriding–dehydriding performance of a 2LiH–MgB2 composite by the catalytic effects of Ni–B nanoparticles. Journal of Materials Chemistry A, 2013, 1, 10184.	5.2	28
57	Enhanced hydrogen storage properties of LiBH4 modified by NbF5. International Journal of Hydrogen Energy, 2014, 39, 11675-11682.	3.8	28
58	Facile synthesis of bowl-like 3D Mg(BH <sub>4</sub> ) <sub>2</sub> –NaBH <sub>4</sub> –fluorographene composite with unexpected superior dehydrogenation performances. Journal of Materials Chemistry A, 2017, 5, 9723-9732.	5.2	28
59	In-situ synthesis of amorphous Mg(BH4)2 and chloride composite modified by NbF5 for superior reversible hydrogen storage properties. International Journal of Hydrogen Energy, 2020, 45, 2044-2053.	3.8	28
60	Extreme high reversible capacity with over 8.0Âwt% and excellent hydrogen storage properties of MgH2 combined with LiBH4 and Li3AlH6. Journal of Energy Chemistry, 2020, 50, 296-306.	7.1	28
61	Tuning electrolyte enables microsized Sn as an advanced anode for Li-ion batteries. Journal of Materials Chemistry A, 2021, 9, 1812-1821.	5.2	28
62	Hydrogen storage performance of 5LiBH4Â+ÂMg2FeH6 composite system. International Journal of Hydrogen Energy, 2012, 37, 6733-6740.	3.8	27
63	Ternary perovskite cobalt titanate/graphene composite material as long-term cyclic anode for lithium-ion battery. Journal of Alloys and Compounds, 2017, 700, 54-60.	2.8	27
64	Fluorographene nanosheets enhanced hydrogen absorption and desorption performances of magnesium hydride. International Journal of Hydrogen Energy, 2014, 39, 12715-12726.	3.8	26
65	Highly efficient ZrH2 nanocatalyst for the superior hydrogenation kinetics of magnesium hydride under moderate conditions: Investigation and mechanistic insights. Applied Surface Science, 2021, 541, 148375.	3.1	26
66	Insights into 2D graphene-like TiO2 (B) nanosheets as highly efficient catalyst for improved low-temperature hydrogen storage properties of MgH2. Materials Today Energy, 2020, 16, 100411.	2.5	25
67	Enhanced hydrogen storage properties of high-loading nanoconfined LiBH4–Mg(BH4)2 composites with porous hollow carbon nanospheres. International Journal of Hydrogen Energy, 2021, 46, 852-864.	3.8	25
68	Enhanced hydrogen desorption properties of LiBH4–Ca(BH4)2 by a synergetic effect of nanoconfinement and catalysis. International Journal of Hydrogen Energy, 2016, 41, 17462-17470.	3.8	24
69	Building robust architectures of carbon-wrapped transition metal nanoparticles for high catalytic enhancement of the 2LiBH <sub>4</sub> -MgH <sub>2</sub> system for hydrogen storage cycling performance. Nanoscale, 2016, 8, 14898-14908.	2.8	24
70	Study on low-vanadium Ti–Zr–Mn–Cr–V based alloys for high-density hydrogen storage. International Journal of Hydrogen Energy, 2022, 47, 1710-1722.	3.8	24
71	Thermodynamics, Kinetics, and Modeling Investigation on the Dehydrogenation of CeAl <sub>4</sub> -Doped NaAlH <sub>4</sub> Hydrogen Storage Material. Journal of Physical Chemistry C, 2011, 115, 22680-22687.	1.5	23
72	A low temperature mechanochemical synthesis and characterization of amorphous Ni–B ultrafine nanoparticles. Materials Letters, 2013, 109, 203-206.	1.3	23

#	Article	IF	CITATIONS
73	Study on the dehydrogenation properties and reversibility of Mg(BH4)2AlH3 composite under moderate conditions. International Journal of Hydrogen Energy, 2017, 42, 8050-8056.	3.8	23
74	GeP5/C composite as anode material for high power sodium-ion batteries with exceptional capacity. Journal of Alloys and Compounds, 2018, 744, 15-22.	2.8	23
75	Remarkable enhancement in dehydrogenation properties of Mg(BH4)2 modified by the synergetic effect of fluorographite and LiBH4. International Journal of Hydrogen Energy, 2015, 40, 14163-14172.	3.8	22
76	In situ synthesis of ultrasmall SnO2 quantum dots on nitrogen-doped reduced graphene oxide composite as high performance anode material for lithium-ion batteries. Journal of Alloys and Compounds, 2017, 727, 1-7.	2.8	22
77	Electrochemical properties of amorphous Mg–Fe alloys mixed with Ni prepared by ball-milling. Journal of Alloys and Compounds, 2006, 413, 312-318.	2.8	21
78	Reversible hydrogen storage behaviors and microstructure of TiC-doped sodium aluminum hydride. Journal of Materials Science, 2009, 44, 4700-4704.	1.7	21
79	Influence of Fe content on the microstructure and hydrogen storage properties of Ti16Zr5Cr22V57ⰒxFex (x=2–8) alloys. International Journal of Hydrogen Energy, 2010, 35, 8143-8148.	3.8	21
80	Fast hydrogen release under moderate conditions from NaBH <sub>4</sub> destabilized by fluorographite. RSC Advances, 2013, 4, 2550-2556.	1.7	21
81	Composite cooperative enhancement on the hydrogen desorption kinetics of LiBH4 by co-doping with NbCl5 and hexagonal BN. International Journal of Hydrogen Energy, 2015, 40, 10527-10535.	3.8	21
82	Ternary perovskite nickel titanate/reduced graphene oxide nano-composite with improved lithium storage properties. RSC Advances, 2016, 6, 61312-61318.	1.7	21
83	La2O3-modified highly dispersed AuPd alloy nanoparticles and their superior catalysis on the dehydrogenation of formic acid. International Journal of Hydrogen Energy, 2017, 42, 9353-9360.	3.8	21
84	The dehydrogenation kinetics and reversibility improvements of Mg(BH4)2 doped with Ti nano-particles under mild conditions. International Journal of Hydrogen Energy, 2021, 46, 23737-23747.	3.8	20
85	Investigation on the nature of active species in the CeCl3-doped sodium alanate system. Journal of Alloys and Compounds, 2011, 509, S750-S753.	2.8	19
86	Superior dehydrogenation performance of nanoscale lithium borohydride modified with fluorographite. International Journal of Hydrogen Energy, 2014, 39, 896-904.	3.8	19
87	Influence of annealing treatment on the microstructure and hydrogen storage performance of Ti1.02Cr1.1Mn0.3Fe0.6 alloy for hybrid hydrogen storage application. Journal of Alloys and Compounds, 2015, 636, 117-123.	2.8	19
88	Rational design of Sn-Sb-S composite with yolk-shell hydrangea-like structure as advanced anode material for sodium-ion batteries. Journal of Alloys and Compounds, 2019, 793, 620-626.	2.8	19
89	Superior catalysis of NbN nanoparticles with intrinsic multiple valence on reversible hydrogen storage properties of magnesium hydride. International Journal of Hydrogen Energy, 2021, 46, 814-822.	3.8	19
90	0D/1D/2D Co@Co2Mo3O8 nanocomposite constructed by mutual-supported Co2Mo3O8 nanosheet and Co nanoparticle: Synthesis and enhanced hydrolytic dehydrogenation of ammonia borane. Chemical Engineering Journal, 2022, 431, 133697.	6.6	19

#	Article	IF	CITATIONS
91	Ultrahigh reversible hydrogen capacity and synergetic mechanism of 2LiBH4-MgH2 system catalyzed by dual-metal fluoride. Chemical Engineering Journal, 2022, 433, 134482.	6.6	19
92	Effect of Ni content on the electrochemical performance of the ball-milled La2Mg17â^'xNix+200wt.% Ni (x=0, 1, 3, 5) composites. Journal of Alloys and Compounds, 2007, 428, 338-343.	2.8	18
93	Hydrogen storage behaviors and microstructure of MF3 (M=Ti, Fe)-doped magnesium hydride. Transactions of Nonferrous Metals Society of China, 2010, 20, 1879-1884.	1.7	18
94	Formation mechanism of MgB2 in 2LiBH4 + MgH2 system for reversible hydrogen storage. Transactions of Nonferrous Metals Society of China, 2011, 21, 1040-1046.	1.7	18
95	A comparative study of the hydrogen storage properties of LiBH4 doping with CaHCl and CaH2. Journal of Alloys and Compounds, 2012, 539, 103-107.	2.8	18
96	Superior Reversible Hydrogen Storage Properties and Mechanism of LiBH <sub>4</sub> –MgH <sub>2</sub> –Al Doped with NbF <sub>5</sub> Additive. Journal of Physical Chemistry C, 2018, 122, 7613-7620.	1.5	18
97	Study on the modification of Zr-Mn-V based alloys for hydrogen isotopes storage and delivery. Journal of Alloys and Compounds, 2019, 797, 185-193.	2.8	18
98	PdCoNi nanoparticles supported on nitrogen-doped porous carbon nanosheets for room temperature dehydrogenation of formic acid. International Journal of Hydrogen Energy, 2019, 44, 11675-11683.	3.8	18
99	LiAlH <sub>4</sub> as a "Microlighter―on the Fluorographite Surface Triggering the Dehydrogenation of Mg(BH <sub>4</sub> ) <sub>2</sub> : Toward More than 7 wt % Hydrogen Release below 70 °C. ACS Applied Energy Materials, 2020, 3, 3033-3041.	2.5	18
100	Achieving excellent cycle stability in Zr–Nb–Co–Ni based hydrogen isotope storage alloys by controllable phase transformation reaction. Renewable Energy, 2022, 187, 500-507.	4.3	18
101	Microstructures and electrochemical hydrogen storage properties of novel Mg–Al–Ni amorphous composites. Electrochemistry Communications, 2009, 11, 515-518.	2.3	17
102	Significantly enhanced hydrogen desorption properties of Mg(AlH4)2 nanoparticles synthesized using solvent free strategy. Progress in Natural Science: Materials International, 2017, 27, 112-120.	1.8	17
103	Facile formation of NiCo2O4 yolk-shell spheres for highly reversible sodium storage. Journal of Alloys and Compounds, 2019, 800, 125-133.	2.8	17
104	The functioning mechanism of Al valid substitution for Co in improving the cycling performance of Zr–Co–Al based hydrogen isotope storage alloys. Journal of Alloys and Compounds, 2020, 848, 156618.	2.8	17
105	Heterostructured Ni/NiO Nanoparticles on 1D Porous MoO <sub><i>x</i></sub> for Hydrolysis of Ammonia Borane. ACS Applied Energy Materials, 2021, 4, 1208-1217.	2.5	17
106	Influence of temperature and hydrogen pressure on the hydriding/dehydriding behavior of Ti-doped sodium aluminum hydride. International Journal of Hydrogen Energy, 2007, 32, 3954-3958.	3.8	16
107	The effect of Cr content on the structural and hydrogen storage characteristics of Ti10V80â^'xFe6Zr4Crx (x=0–14) alloys. Journal of Alloys and Compounds, 2010, 493, 396-400.	2.8	16
108	Comprehensive hydrogen storage properties and catalytic mechanism studies of 2LiBH4–MgH2 system with NbF5 in various addition amounts. International Journal of Hydrogen Energy, 2014, 39, 7050-7059.	3.8	16

#	Article	IF	CITATIONS
109	Dual-Ion Substitution-Induced Unique Electronic Modulation to Stabilize an Orthorhombic Lattice towards Reversible Hydrogen Isotope Storage. ACS Sustainable Chemistry and Engineering, 2021, 9, 9139-9148.	3.2	16
110	Effects of ball-milling time and Bi2O3 addition on electrochemical performance of ball-milled La2Mg17+200wt.% Ni composites. Journal of Alloys and Compounds, 2006, 416, 194-198.	2.8	15
111	Probing an intermediate state by X-ray absorption near-edge structure in nickel-doped 2LiBH4–MgH2 reactive hydride composite at moderate temperature. Materials Today Nano, 2020, 12, 100090.	2.3	15
112	Improved reversible dehydrogenation properties of Mg(BH4)2 catalyzed by dual-cation transition metal fluorides K2TiF6 and K2NbF7. Chemical Engineering Journal, 2021, 412, 128738.	6.6	15
113	Hydriding/dehydriding behaviors of La1.8Ca0.2Mg14Ni3 alloy modified by mechanical ball-milling under argon. Journal of Alloys and Compounds, 2005, 399, 178-182.	2.8	14
114	Enhanced reversible hydrogen desorption properties and mechanism of Mg(BH4)2-AlH3-LiH composite. Journal of Alloys and Compounds, 2018, 762, 548-554.	2.8	14
115	Facile synthesis of AuPd nanoparticles anchored on TiO2 nanosheets for efficient dehydrogenation of formic acid. Nanotechnology, 2018, 29, 335402.	1.3	14
116	Enhancing the reversibility of SnCoS4 microflower for sodium-ion battery anode material. Journal of Alloys and Compounds, 2020, 825, 154104.	2.8	14
117	Synergetic Effect of in Situ Formed Nano NbH and LiH <sub>1–<i>x</i></sub> F <sub><i>x</i></sub> for Improving Reversible Hydrogen Storage Properties of the Li–Mg–B–H System. Journal of Physical Chemistry C, 2013, 117, 12019-12025.	1.5	13
118	Electrode properties of La2Mg17 alloy ball-milled with xwt.% cobalt powder (x=50, 100, 150 and 200). Journal of Alloys and Compounds, 2006, 414, 248-252.	2.8	12
119	Synthesis and hydriding/dehydriding properties of nanosized sodium alanates prepared by reactive ball-milling. International Journal of Hydrogen Energy, 2011, 36, 539-548.	3.8	12
120	Investigation on synthesis, structure and catalytic modification of Ca(AlH4)2 complex hydride. International Journal of Hydrogen Energy, 2012, 37, 936-941.	3.8	12
121	Improved de/hydrogenation properties and favorable reaction mechanism of CeH2Â+ÂKH co-doped sodium aluminum hydride. International Journal of Hydrogen Energy, 2014, 39, 6577-6587.	3.8	12
122	Synthesis of nanoscale CeAl4 and its high catalytic efficiency for hydrogen storage of sodium alanate. Rare Metals, 2017, 36, 77-85.	3.6	12
123	Regulating local chemistry in ZrCo-based orthorhombic hydrides via increasing atomic interference for ultra-stable hydrogen isotopes storage. Journal of Energy Chemistry, 2022, 69, 397-405.	7.1	12
124	Dynamically Staged Phase Transformation Mechanism of Co-Containing Rare Earth-Based Metal Hydrides with Unexpected Hysteresis Amelioration. ACS Applied Energy Materials, 2022, 5, 3783-3792.	2.5	12
125	Synthesis and dehydrogenation of CeAl4-doped calcium alanate. Journal of Alloys and Compounds, 2011, 509, S743-S746.	2.8	11
126	Superior Catalytic Effects of Transition Metal Boride Nanoparticles on the Reversible Hydrogen Storage Properties of Liâ€Mgâ€Bâ€H System. Particle and Particle Systems Characterization, 2014, 31, 195-200.	1.2	11

#	Article	IF	CITATIONS
127	Significantly improved de/rehydrogenation properties of lithium borohydride modified with hexagonal boron nitride. RSC Advances, 2015, 5, 51110-51115.	1.7	11
128	Enhanced hydrogen storage properties of a dual-cation (Li <sup>+</sup> , Mg <sup>2+</sup> ) borohydride and its dehydrogenation mechanism. RSC Advances, 2017, 7, 36852-36859.	1.7	11
129	A new strategy to remarkably improve the low-temperature reversible hydrogen desorption performances of LiBH4 by compositing with fluorographene. International Journal of Hydrogen Energy, 2017, 42, 20046-20055.	3.8	11
130	Dehydrogenation Performances of Different Al Source Composite Systems of 2LiBH4 + M (M = Al,) Tj ETQq0 0 0	rgBT /Ove 1.8	erlock 10 Tf 50
131	A dandelion-like amorphous composite catalyst with outstanding performance for sodium borohydride hydrogen generation. International Journal of Hydrogen Energy, 2021, 46, 10809-10818.	3.8	11
132	Studies on Ti-Zr-Cr-Mn-Fe-V based alloys for hydrogen compression under mild thermal conditions of water bath. Journal of Alloys and Compounds, 2022, 892, 162145.	2.8	11
133	Synthesis of calcium alanate and its dehydriding performance enhanced by FeF3 doping. Journal of Alloys and Compounds, 2011, 509, 590-595.	2.8	10
134	Effects of Fluoride Additives on the Hydrogen Storage Performance of 2LiBH <sub>4</sub> –Li <sub>3</sub> AlH <sub>6</sub> Destabilized System. Journal of Physical Chemistry C, 2012, 116, 22226-22230.	1.5	10
135	Enhanced reversible hydrogen storage performance of NbCl5 doped 2LiH–MgB2 composite. International Journal of Hydrogen Energy, 2014, 39, 2132-2141.	3.8	10
136	Development of Ti0.85Zr0.17(Cr-Mn-V)1.3Fe0.7-based Laves phase alloys for thermal hydrogen compression at mild operating temperatures. Rare Metals, 2022, 41, 2588-2594.	3.6	10
137	Soft chemical synthesis and characterization of lithium nickel oxide electrode materials. Journal of Materials Science, 1996, 31, 6449-6454.	1.7	9
138	Effects of Ti-based additives on Mg2FeH6 dehydrogenation properties. Transactions of Nonferrous Metals Society of China, 2016, 26, 791-798.	1.7	9
139	Effects of supplementing sow diets with Saccharomyces cerevisiae refermented sorghum dried distiller's grains with solubles from late gestation to weaning on the performance of sows and progeny1. Journal of Animal Science, 2017, 95, 2025-2031.	0.2	9
140	In-situ formation of ultrafine MgNi3B2 and TiB2 nanoparticles: Heterogeneous nucleating and grain coarsening retardant agents for magnesium borate in Li–Mg–B–H reactive hydride composite. International Journal of Hydrogen Energy, 2019, 44, 27529-27541.	3.8	9
141	Excellent Catalysis of Various TiO2 Dopants with Na0.46TiO2 in Situ Formed on the Enhanced Dehydrogenation Properties of NaMgH3. Journal of Physical Chemistry C, 2019, 123, 22832-22841.	1.5	9
142	An impact of hydrogenation phase transformation mechanism on the cyclic stabilizing behavior of Zr0.8Ti0.2Co alloy for hydrogen isotopeÂhandling. Materials Today Energy, 2020, 18, 100554.	2.5	9
143	Ultra-fast dehydrogenation behavior at low temperature of LiAlH4 modified by fluorographite. International Journal of Hydrogen Energy, 2020, 45, 28123-28133.	3.8	9
144	Positive impacts of tuning lattice on cyclic performance in ZrCo-based hydrogen isotopeÂstorage alloys. Materials Today Energy, 2021, 20, 100645.	2.5	9

#	Article	IF	CITATIONS
145	Direct synthesis and hydrogen storage behaviors of nanocrystalline Na2LiAlH6. Journal of Materials Science, 2011, 46, 3314-3318.	1.7	8
146	Influence of lanthanon hydride catalysts on hydrogen storage properties of sodium alanates. Journal of Rare Earths, 2013, 31, 502-506.	2.5	8
147	A Novel Li–Ca–B–H Complex Borohydride: Its Synthesis and Hydrogen Storage Properties. Journal of Physical Chemistry C, 2011, 115, 19986-19993.	1.5	7
148	Enhanced dehydrogenation performances and mechanism of LiBH4/Mg17Al12-hydride composite. Transactions of Nonferrous Metals Society of China, 2014, 24, 152-157.	1.7	7
149	In situ synthesized SnO2 nanorod/reduced graphene oxide low-dimensional structure for enhanced lithium storage. Nanotechnology, 2018, 29, 105705.	1.3	7
150	Influence of TiC catalyst on absorption/desorption behaviors and microstructures of sodium aluminum hydride. Transactions of Nonferrous Metals Society of China, 2011, 21, 1297-1302.	1.7	6
151	Low-cost batteries based on industrial waste Al–Si microparticles and LiFePO <sub>4</sub> for stationary energy storage. Dalton Transactions, 2021, 50, 8322-8329.	1.6	6
152	Hydrogen desorption from MgH2+NH4Cl/graphene composites at low temperatures. Materials Chemistry and Physics, 2021, 263, 124342.	2.0	6
153	Microstructure and hydrogen storage properties of Ti10+V80-Fe6Zr4 (x=0~15) alloys. International Journal of Hydrogen Energy, 2021, 46, 27622-27630.	3.8	5
154	Effect of quenching treatment on the phase structure and electrochemical properties of V2.1TiNi0.4Zr0.06Mn0.05 alloy. International Journal of Hydrogen Energy, 2009, 34, 7756-7760.	3.8	4
155	Insights into magnesium borohydride dehydrogenation mechanism from its partial reversibility under moderate conditions. Materials Today Energy, 2020, 18, 100552.	2.5	4
156	Enhancing Hydrogen Storage Kinetics and Cycling Properties of NaMgH3 by 2D Transition Metal Carbide MXene Ti3C2. Processes, 2021, 9, 1690.	1.3	4
157	Effects of surface modification on the electrode behavior of ball-milled La2Mg17+200wt% Ni composite in alkaline solution. Journal of Alloys and Compounds, 2006, 420, 306-311.	2.8	3
158	Dehydriding properties of Ti or/and Zr-doped sodium aluminum hydride prepared by ball-milling. Physica Scripta, 2007, T129, 95-98.	1.2	2
159	Influence of KH on Reversible Dehydriding Performance of Na-Al-H Complex Hydride. Wuli Huaxue Xuebao/ Acta Physico - Chimica Sinica, 2013, 29, 1804-1808.	2.2	0
160	Optoelectronic Devices: Lowâ€Temperature Combustionâ€Synthesized Nickel Oxide Thin Films as Holeâ€Transport Interlayers for Solutionâ€Processed Optoelectronic Devices (Adv. Energy Mater. 6/2014). Advanced Energy Materials, 2014, 4, .	10.2	0
161	Functional Nanomaterials for Renewable Energy and Sustainability. Journal of Nanomaterials, 2017, 2017, 1-1.	1.5	0